JOC The Journal of Organic Chemistry

Article

Structure#Property Relationships of Stable Free Radicals: Verdazyls with Electron-Rich Aryl Substituents

Victoria Chemistruck, Dallas Chambers, and David J. R. Brook

J. Org. Chem., **2009**, 74 (5), 1850-1857• DOI: 10.1021/jo8019829 • Publication Date (Web): 05 February 2009

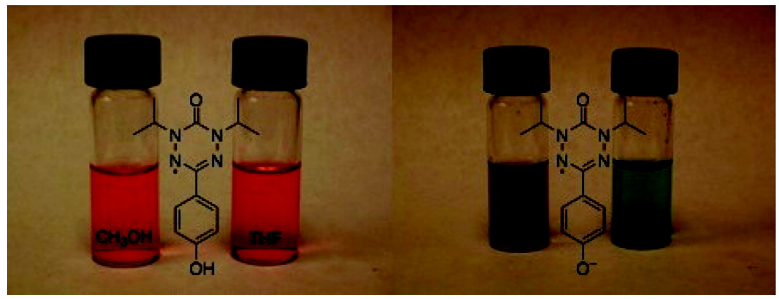

JOC Article

Structure−Property Relationships of Stable Free Radicals: Verdazyls with Electron-Rich Aryl Substituents

Victoria Chemistruck, Dallas Chambers, and David J. R. Brook*

Department of Chemistry, San José State University, One Washington Square, San José, California 95192

dbrook@science.sjsu.edu

Received September 8, 2008

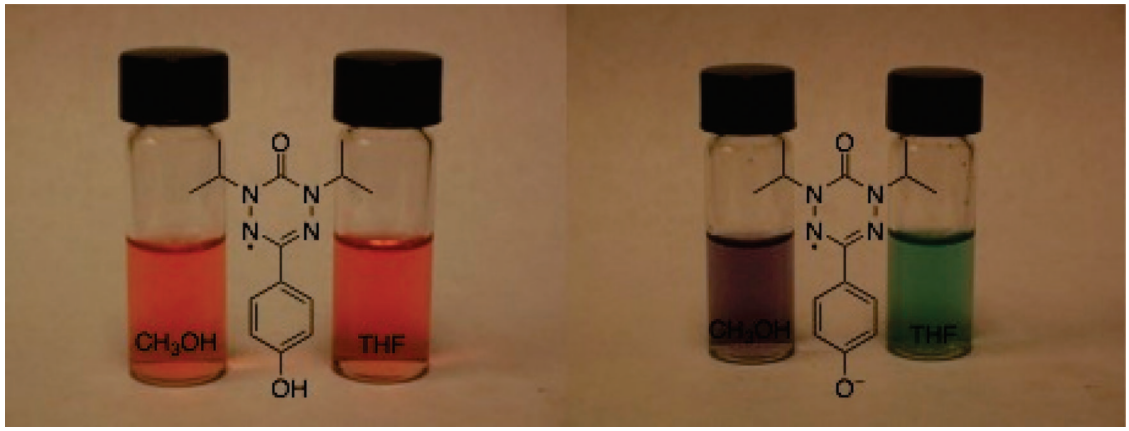

Substitution of the 3 position of 6-oxoverdazyl free radicals with electron-rich arylamines, phenols, and aryl ethers elicits changes in the UV−vis spectra and in the pK_a of the aryl substituents consistent with the verdazyl being electron withdrawing. The pK_a of substituents is decreased: in 80% methanol phenols **3a** and **3b** have pK_a of 10.4 and 10.9, respectively, while the ammonium ion from protonation of **3j** has pK_a = 2.4. On the basis of these measurements, Hammett parameters for the verdazyl have been estimated: $\sigma_p^- = +0.48$ and $\sigma_m = +0.27$. The longest wavelength band in the visible spectrum is red-shifted with increasingly electron-rich aromatic rings and with increasingly polar solvents, consistent with a transition from the highest fully occupied orbital to the radical SOMO. Exceptions occur when additional interactions occur between verdazyl and substituent; hydrogen bonding in the case of **3c** and steric interference for **3f.** Measurements such as ESR and electrochemistry that are dependent largely on the SOMO are relatively insensitive to changes in substituent.

Introduction

Stable free radicals have intrinsic fundamental importance in organic chemistry as a result of their unusual electronic structure. The presence of an unpaired electron also facilitates their application as spin labels and components of magnetic materials both on their own and coordinated with metal ions.[1] Furthermore their propensity for one-electron redox chemistry enables their use as charge storage components in batteries,[2−7] and combined with other chromophores they provide the basis for a variety of novel molecular probes and switchable organic materials.[8,9] Control and understanding of the role free radicals play in these applications requires a knowledge of the electronic structure of the radicals and how they interact with neighboring groups and coordinated metal ions. In particular, we are interested in understanding how free radicals may interact with and perturb other functional groups. With a half-filled non-

(1) Lahti, P. M. In *Molecular Magnetism in Organic-Based Materials*; Marcel-Dekker: New York, 1999; p *728*.
(2) Nishide, H.; Iwasa, S.; Pu, Y.; Suga, T.; Nakahara, K.; Satoh, M. *Electrochim. Acta* **2004**, *50*, 827–831.
(3) Suga, T.; Konishi, H.; Nishide, H. *Chem. Commun.* **2007**, 1730–1732.
(4) Kim, J.; Cheruvally, G.; Choi, J.; Ahn, J.; Lee, S. H.; Choi, D. S.; Song, C. E. *Solid State Ionics* **2007**, *178*, 1546–1551.
(5) Bugnon, L.; Morton, C. J. H.; Novak, P.; Vetter, J.; Nesvadba, P. *Chem. Mater.* **2007**, *19*, 2910–2914.
(6) Qu, J.; Morita, R.; Satoh, M.; Wada, J.; Terakura, F.; Mizoguchi, K.; Ogata, N.; Masuda, T. *Chem. Eur. J.* **2008**, *14*, 3250–3259.
(7) Katstumata, T.; Qu, J.; Shiotsuki, M.; Satoh, M.; Wada, J.; Igarashi, J.; Mizoguchi, K.; Masuda, T. *Macromolecules* **2008**, *41*, 1175–1183.
(8) Likhtenstein, G. I.; Ishii, K.; Nakatsuji, S. *Photochem. Photobiol.* **2007**, *83*, 871–881.

10.1021/jo8019829 CCC: $40.75
Published on Web 02/05/2009

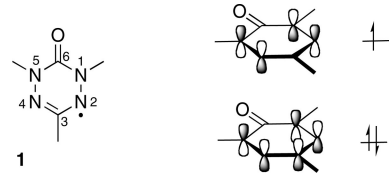

FIGURE 1. Structure and numbering of verdazyl radicals, and cartoon representation of the highest occupied orbitals.

bonding orbital, a particular free radical may act as an electron donor, electron acceptor, or possibly even both. Substituents on a free radical may interact with both the singly occupied orbital and HOMO and LUMO orbitals, potentially stabilizing or destabilizing the radical. Predicting the exact nature and extent of these interactions depends on understanding the precise radical structure, which may in turn be probed by examining the physical and spectroscopic properties of both radical and substituent.

Among stable free radicals, 6-oxoverdazyls **1** (Figure 1) have gained interest because of their ability to coordinate metal ions through nitrogen giving strong magnetic interactions,[10−14] their potential structural variability, and also because of the possibility of radical mediating interactions between the multiple substituents on the verdazyl ring. Synthetically, the 3 position in the 6-oxoverdazyl structure is the easiest to vary. The 3 position of the verdazyl is also the site of a node in the SOMO (Figure 1), so substituents in this position have little direct effect on the radical itself. This is reflected in the ESR spectra[15] and electrochemical properties.[16] Nevertheless, effects of the verdazyl on the substituent itself may still be apparent—for example, we may see changes in substituent pK_a, or in the UV−vis spectrum of the verdazyls. Understanding the UV−visible spectra is especially important since it provides a direct window into the electronic structure of these species and may facilitate the understanding of verdazyl coordination compounds and the design of radical-based organic devices.

To address some of these questions we have synthesized a series of new donor-substituted verdazyls. We report the characterization of these and some previously reported species, particularly in terms of pK_a, electrochemistry, and UV−visible spectroscopy, and discuss their physical properties in terms of the radical−substituent interaction. We also discuss the implications for further development and application of verdazyl chemistry.

Results

Ten different verdazyls **3a**−**j** were studied (Scheme 1). The 2′- and 4′-hydroxyphenylverdazyls (**3a** and **3c**) have been reported previously.[15] The remaining verdazyls with the exception of **3d** were synthesized by oxidation of the corresponding

SCHEME 1. Synthesis of Oxophenyl and Aminophenyl-Substituted Verdazyl Radicals

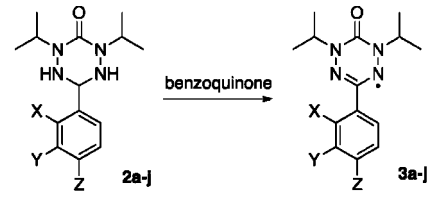

	X	Y	Z
a	H	H	OH
b	H	OH	H
c	OH	H	H
d	H	H	OCH_3
e	H	OCH_3	H
f	OCH_3	H	H
g	H	OH	OH
h	H	OCH_3	OH
i	H	OCH_3	OCH_3
j	H	H	$(CH_3)_2N$

tetrazanes **2a**−**j** with benzoquinone (Scheme 1)[15] The 4-methoxyphenylverdazyl **3d** was synthesized by methylating the corresponding phenol by using cesium carbonate and methyl iodide in dimethyl formamide.

All of the verdazyls studied are yellow to red crystalline solids and are stable in air at ambient temperatures. ESR spectra of all free radicals were almost identical with those reported for other 1,5-diisopropyl verdazyls.[15] Hyperfine parameters are listed in the Supporting Information. The verdazyl structure was also confirmed by single-crystal X-ray diffraction on the 4-hydroxyphenyl verdazyl **3a** and the 2-methoxyphenyl verdazyl **3f.** Bond lengths and angles within the verdazyl were found to be consistent with earlier studies[17] and are also provided in the Supporting Information. Of particular importance is the angle between the planes of the verdazyl and phenyl rings. For **3a** the angle is 26°, but in **3f** steric interaction with the methoxy substituent increases the angle to 61°. Thermal ellipsoid plots of both structures are shown in Figure 2.

In solution the neutral verdazyls are yellow to red depending upon the type and position of the substituents. Similar to other reported 3-aryl-6-oxoverdayls, most of the UV−visible spectra show two overlapping bands with maxima typically near 420 and 500 nm. The position of the latter band varies significantly with changes in substituent (including deprotonation of phenols **3a**−**c** or protonation of amine **3j**). Maxima and extinction coefficients are listed in Table 1 while representative UV−visible spectra of both are shown in Figure 3a−d.

To gain further insight into the UV−vis spectra, the energy of the two visible bands is plotted against Hammett constant (σ_p or σ_m values from ref 27) in Figure 4. In addition UV−vis spectra of **3j** and the anion of **3a** (for which solvent effects are most pronounced) were recorded in a variety of protic and aprotic solvents. Plots of the energy of the longest wavelength band vs solvent polarity (as measured by the solvent parameter

(9) Hicks, R. G. *Org. Biomol. Chem.* **2007**, *5*, 1321–1338.
(10) Barclay, T. M.; Hicks, R. G.; Lemaire, M. T.; Thompson, L. K. *Inorg. Chem.* **2001**, *40*, 5581–5584.
(11) Barclay, T. M.; Hicks, R. G.; Lemaire, M. T.; Thompson, L. K. *Chem. Commun.* **2000**, 2141.
(12) Barclay, T. M.; Hicks, R. G.; Lemaire, M. T.; Thompson, L. K.; Xu, Z. Q. *Chem. Commun.* **2002**, 1688–1689.
(13) Hicks, R. G.; Lemaire, M. T.; Thompson, L. K.; Barclay, T. M. *J. Am. Chem. Soc.* **2000**, *122*, 8077–8079.
(14) Norel, L.; Pointillart, F.; Train, C.; Chamoreau, L.; Boubekeur, K.; Journaux, Y.; Brieger, A.; Brook, D. J. R. *Inorg. Chem.* **2008**, *47*, 2396–2403.
(15) Paré, E. C.; Brook, D. J. R.; Brieger, A.; Badik, M.; Schinke, M. *Org. Biomol. Chem.* **2005**, *3*, 4258–4261.
(16) Gilroy, J. B.; McKinnon, S. D. J.; Koivisto, B. D.; Hicks, R. G. *Org. Lett.* **2007**, *9*, 4837–4840.
(17) Brook, D. J. R.; Yee, G. T. *J. Org. Chem.* **2006**, *71*, 4889–4895.

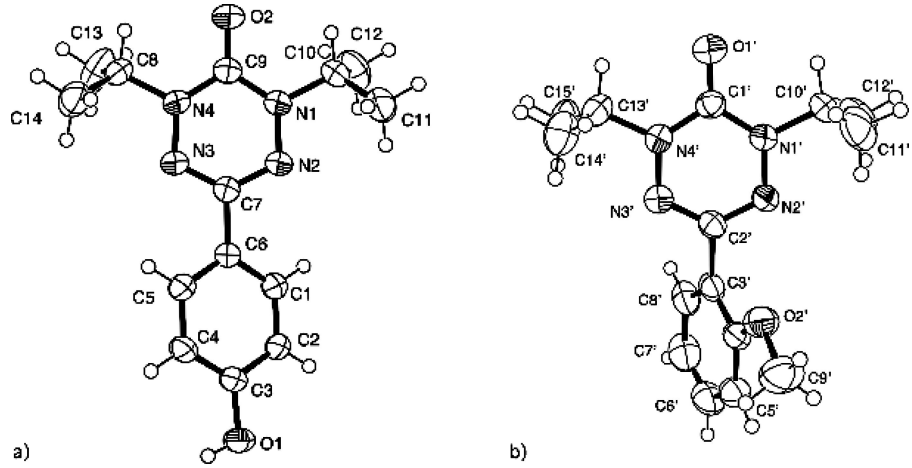

FIGURE 2. Thermal ellipsoid plots of **3a** (a) and **3f** (b). Only one of the two crystallographically independent molecules of **3f** is shown. Ellipsoids are drawn at the 50% level.

TABLE 1. UV−Vis Maxima for Radicals 3a−j in Acetonitrile

radical/substituent	$\lambda_{1,max}$/nm ($\varepsilon_{1,max}$/L mol^{-1} cm^{-1})	$\lambda_{2,max}$/nm ($\varepsilon_{2,max}$/L mol^{-1} cm^{-1})
3a/4′-OH	419 (1020)	515 (520)
3b/3′-OH	414 (1010)	490 (470)
3c/2′-OH	425 (1300)	525 (600)
3d/4′-OCH_3	418 (700)	496, 515 (305)
3e/3′-OCH_3	414 (1530)	491 (520)
3f/2′-OCH_3	492 (1150)	445 (830)
3g/3′,4′-$(OH)_2$	420 (970)	520 (460)
3h/3′-(OCH_3)-4′-OH	423 (1000)	528 (530)
3i/3′,4′-$(OCH_3)_2$	422 (900)	523 (450)
3j/4′-$N(CH_3)_2$	425 (470)	569 (370)
3j-H^+/4′-$NH(CH_3)_2^+$	412 (1880)	466 (506)

π^*) and hydrogen bond donor ability α (for solvents with nonzero α) are shown in Figure 5.

Solutions of the phenolic verdazyls **3a−c** and the amino verdazyl **3j** in buffered 80% (w/w) methanol/water were titrated with NaOH and/or HCl. Analysis of the UV−vis spectra as a function of corrected pH[18] provided the pK_a values listed in Table 2. Full sets of titration data are shown in the Supporting Information.

Cyclic voltammetry was recorded on all verdazyls in acetonitrile. An internal ferrocene standard was used and potentials were corrected to SCE. All species showed reversible one-electron oxidation waves near +0.6 V vs SCE. In addition verdazyls without acidic hydrogens showed reversible one-electron reduction, and in some cases, a second reversible wave corresponding to oxidation of the donor substituted benzene ring. For most of the phenols (**3a−c**,**g** but not **3h**) an irreversible reduction wave was generally associated with a poorly defined return oxidation near +0.2 V vs SCE. At positive potentials an irreversible wave associated with oxidation of the phenol was observed. Details are provided in Table 3.

Discussion

As noted in the introduction, the verdazyl SOMO has a node at the 3 position of the ring. This means that the SOMO is relatively insensitive to substituents at the 3 position. Furthermore, properties largely dependent on the SOMO, such as ESR spectra and oxidation potentials, show the same insensitivity. Consistent with this, the ESR spectra of all the radicals studied are very similar to those reported for other diisopropyl verdazyl free radicals.[17] A similar phenomenon was noted for a series of nitronyl nitroxides, where even very small changes in hyperfine coupling to hydrogens on the phenyl ring could not be attributed to resonance effects such as the position of the substituent.[24]

Similarly, a recent article by Hicks and co-workers discussed the electrochemistry of verdazyls[16] and noted that substituent effects at the 3 position of the verdazyl were small. As reference species, both 1,5-diisopropyl-3-phenylverdazyl and 1,5-diisopropyl-3-methyl verdazyls have oxidation potentials $E°(V^{\bullet}/V^+)$ of +0.6 V vs SCE (Table 3).[16,17,25] Electron-deficient pyridyl and imidazolyl heterocycles at the 3 position increase $E°(V^{\bullet}/V^+)$ by 0.04−0.06V.[16] The verdazyls in this study, with electron-rich phenyl groups at the 3 position, generally give slightly lower $E°(V^{\bullet}/V^+)$ (by up to 0.08 V) though within this group it is hard to find meaningful correlations. The 2′-methoxyphenyl verdazyl shows no conjugation between the phenyl ring and the verdazyl, so it is not surprising that $E°(V^{\bullet}/V^+)$ is unchanged, but only small ($\leq$0.01V) changes in $E°(V^{\bullet}/V^+)$ are observed for the 3′-hydroxyphenyl and 4′-hydroxyphenyl radicals **3a**,**b** and the dimethoxyphenyl radical **3i**. The 3′-substituted radicals **3b** and **3e** have slightly higher $E°(V^{\bullet}/V^+)$ than their 4′-counterparts which may be consistent with a loss of resonance interaction between the substituent and verdazyl. Strangely, however, the 3′-methoxyphenyl and 4′-methoxyphenyl radicals **3d**,**e** are easier to oxidize than their hydroxy counterparts **3a**,**b** and the dimethylaminophenyl radical **3j** actually has a *higher* $E°(V^{\bullet}/V^+)$ than the 4-methoxyphenyl **3d**.

These weak and irregular effects cannot be easily explained with a simple model, though their small size is consistent with the orbital model described above. Nevertheless, some variations

(18) Canals, I.; Oumada, F. Z.; Rosés, M.; Bosch, E. *J. Chromatogr. A* **2001**, *911*, 191–202.
(19) Parsons, G. H.; Rochester, C. H. *J. Chem. Soc., Faraday Trans. 1* **1975**, *71*, 1058–1068.
(20) Bacarella, A. L.; Grunwald, E.; Marshall, H. P.; Purlee, E. L. *J. Org. Chem.* **1955**, *20*, 747–762.
(21) Porcal, G.; Bertolotti, S. G.; Previtah, C. M.; Encinas, M. V. *Phys. Chem. Chem. Phys.* **2003**, *5*, 4123–4128.
(22) Williams, L. L.; Webster, R. D. *J. Am. Chem. Soc.* **2004**, *126*, 12441–12450.
(23) Fico, R. M., Jr.; Hay, M. F.; Reese, S.; Hammond, S.; Lambert, E.; Fox, M. A. *J. Org. Chem.* **1999**, *64*, 9386–9392.
(24) Cirujeda, J.; Vidal-Gancedo, J.; Juergens, O.; Mota, F.; Novoa, J. J.; Rovira, C.; Veciana, J. *J. Am. Chem. Soc.* **2000**, *122*, 11393–11405.
(25) Barr, C. L.; Chase, P. A.; Hicks, R. G.; Lemaire, M. T.; Stevens, C. L. *J. Org. Chem.* **1999**, *64*, 8893.

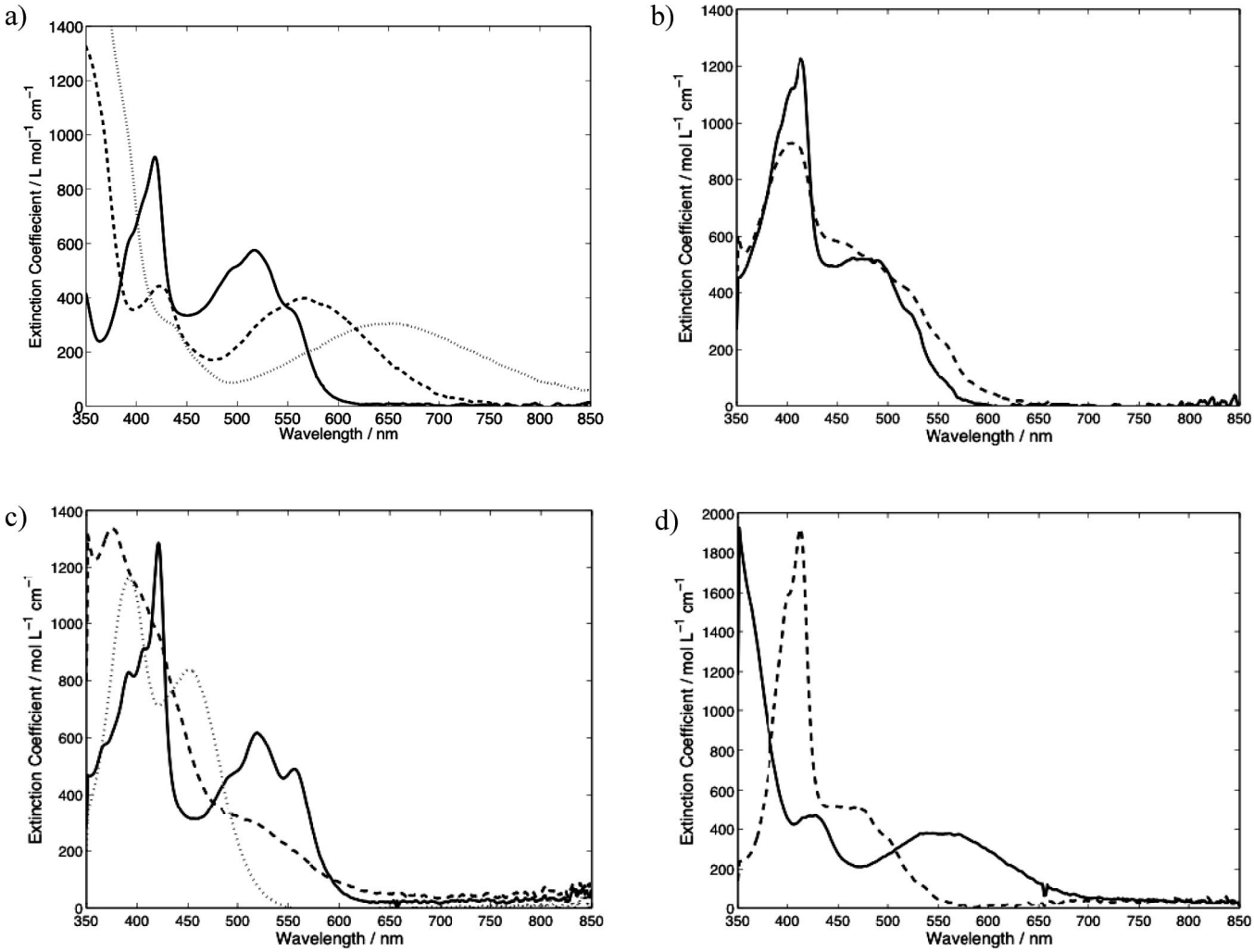

FIGURE 3. (a) UV spectra of **3a** (—) and the corresponding anion in 80% aqueous methanol (---) and acetonitrile (•••). (b) UV−vis spectra of radical **3b** (—) and the corresponding anion (---) in 80% aqueous methanol. (c) UV−vis spectra of radical **3c** (—) and the corresponding anion (---) in 80% aqueous methanol and radical **3f** in acetonitrile (•••). (d) UV−vis spectra of radical **3j** (—) and the corresponding cation (---) in 80% aqueous methanol.

in $E°(V^{\bullet}/V^{+})$ are more easily rationalized. Protonation of the dimethylaminophenyl radical **3j** to form an ammonium cation increases $E°(V^{\bullet}/V^{+})$ by 0.15 V, as a result of both the electron-withdrawing cation and the overal increase in charge. $E°(V^{\bullet}/V^{+})$ for the 2′-hydroxy phenyl radical **3c** is 0.1 V greater than any of the other hydroxyphenyl verdazyls, probably as a result of an intramolecular hydrogen bond that is broken upon oxidation. The presence of this hydrogen bond was confirmed by comparison of the IR spectra of **3a**, **3b**, and **3c** in chloroform solution. Both the 4′- substituted phenol **3a** and the 3′-substituted phenol **3b** give well-resolved, non-hydrogen bonded OH stretches at 3595 cm^{-1} whereas the OH stretch in the 2-substituted species **3c** is at 3413 cm^{-1}.

Comparison of our electrochemical results with those reported earlier for directly linked and methylene bridged verdazyls show that the verdazyl itself is electron withdrawing. This results in increases in $E°(V^{\bullet}/V^{+})$ from 0.05 to 0.1 V. While this also might be revealed in the oxidation potentials of groups attached to the verdazyl ($E°(Ar/Ar^{\bullet+})$), none of the substituents show a clear reversible oxidation before the oxidation of the verdazyl itself. Not surprisingly the verdazylium ion has a stronger electron withdrawing effect than the verdazyl—$E°(Ar/Ar^{\bullet+})$ for **3i** and **3j** occurs 0.1−0.2 V higher than in veratrole and *N*,*N*-dimethylaniline respectively.

The electron-withdrawing effects of the verdazyl ring are more evident in the pK_a measurements (Table 2) and electronic spectra (Figure 3−5 and Table 1). Phenol **3a** has a pK_a between that of *p*-bromophenol and 4-hydroxybenzaldehyde.[19] A plot of phenol pK_a in 80% methanol (where pK_a values in 80% methanol were not available they were calculated[26] from the measured pK_a in water) vs Hammett σ_m/σ_p^- is linear, with correlation coefficient $R = -0.99$ and $\rho = -2.43$. Consequently we can use the pK_a of **3a**,**b** to estimate the Hammett constants σ_m/σ_p^- for a verdazyl substituent. This gives σ_p^-(verdazyl) = +0.48 and σ_m(verdazyl) = +0.27. This compares with other nitrogen heterocycles such as 2-benzoimidazolyl ($\sigma_p^- = +0.48$) and 2-indolyl ($\sigma_p^- = 0.39$)[27] and suggests that the change in pK_a is a result of the heterocyclic structure in general rather than an effect of the unpaired electron. The 2-hydroxyphenol **3c** is less acidic than phenol itself, presumably as a result of the internal hydrogen bond; a similar effect is seen in comparing 4-hydroxybenzaldehyde (pK_a = 9.08 in 80% MeOH) with salicylaldehyde (pK_a = 10.00 in 80% MeOH).[26] Similar to the

(26) Rosés, M.; Rived, F.; Bosch, E. *J. Chromatogr. A* **2000**, *867*, 45–56.

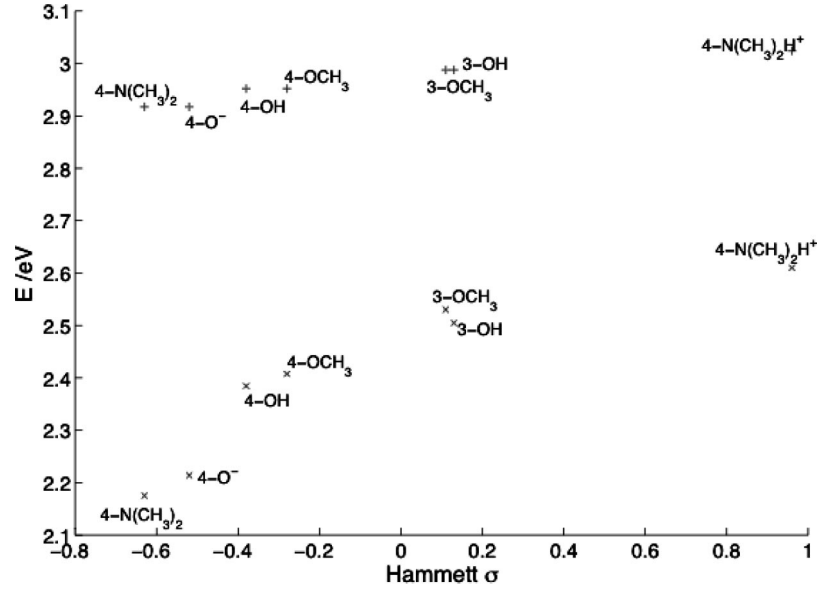

FIGURE 4. Plot of the energy of visible band maxima vs Hammett constant σ_p/σ_m.

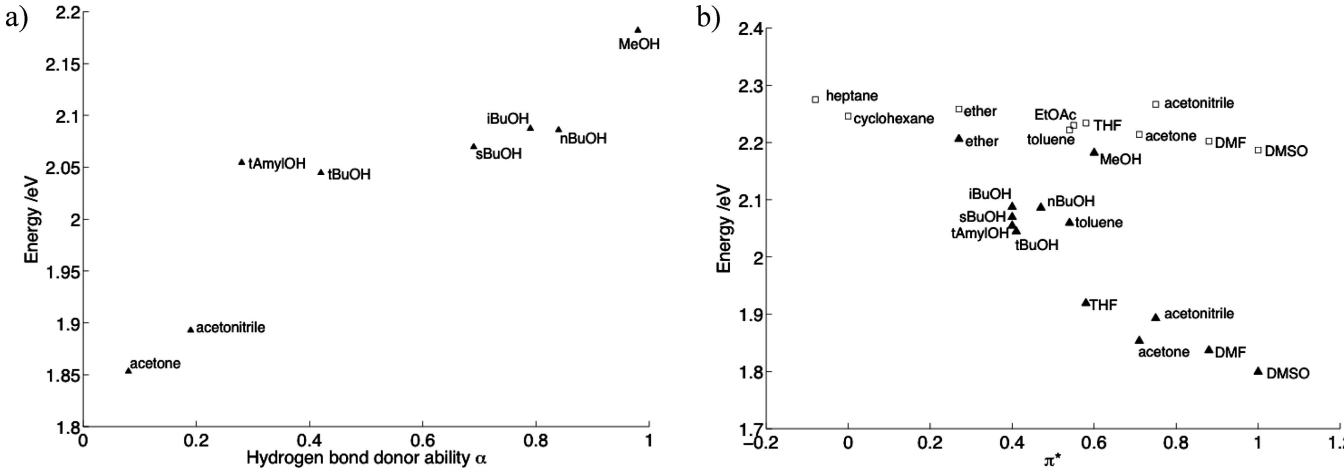

FIGURE 5. (a) Plot of energy of the long wavelength visible band of the anion of **3a** vs hydrogen bond donation ability, α. (b) Plot of energy of the longest wavelength visible band vs π^* for **3j** (squares) and the anion of **3a** (triangles).

TABLE 2. Measured pK_a of Radicals 3a-c, 3j and Comparable Phenols and Ammonium Ions in 80% Methanol/Water

radical/substituent	pK_a
3a/4′-OH	10.4(1)
3b/3′-OH	10.9(1)
3c/2′-OH	12.6(1)
3j-H^+/4′-$NH(CH_3)_2^+$	2.4(1)
phenol	11.63[a]
4-bromophenol	10.86[a]
4-hydroxybenzaldehyde	9.08[a]
N,*N*-dimethylanilinium	3.82[b]

[a] Values from ref 19. [b] Value from ref 20.

phenol **3a**, the ion resulting from protonation of **3j** is more acidic than dimethylanilinium by ~1.5 pK_a units.

In one of our initial reports on coordination chemistry of 6-oxoverdazyls we assigned the two bands in the visible region to n−π^* and $\pi-\pi^*$ transitions respectively based on computational data.[28] On the basis of the current data, these assignments may be incorrect, or at the least, simplistic. For the longest wavelength band, the negative correlation of energy with solvent polarity measured by the π^* solvent scale (Figure 5a) suggests that this is a $\pi-\pi^*$ transition. Furthermore the correlation of energy with Hammett constants σ_p and σ_m (Figure 4) suggests a degree of charge transfer interaction between the aromatic ring and the verdazyl in the excited state; that is, resonance structures such as that depicted in Figure 6 make a contribution to the excited state.

This is further supported by the effect of hydrogen bonding on the anion of **3a**, which stabilizes the phenoxide, reducing its ability to donate electrons and increasing the energy of the transition (Figure 5b). A similar observation was made with Dimroth's dye (**4**) where the absorbance results from a charge transfer from phenolate to pyridinium and the energy of this transition is directly related to the solvation of the phenolate.[29]

These observations collectively suggest a description of the low energy transition in 3-aryl verdazyls as a transition from a π orbital into the verdazyl SOMO. The donor π orbital has an

(27) Exner, O. In *Correlation Analysis in Chemistry: Recent Advances*; Chapman, N. B., Shorter, J., Eds.; Plenum: New York, 1978; p 439.

(28) Brook, D. J. R.; Fornell, S.; Stevens, J. E.; Noll, B.; Koch, T. H.; Eisfeld, W. *Inorg. Chem.* **2000**, *39*, 562.

(29) Coleman, C. A.; Murray, C. J. *J. Org. Chem.* **1992**, *57*, 3578–3582.

TABLE 3. Electrochemistry of Radicals 3a−j and Related Species[f]

Radical / Substituent	$E^\circ(V^\bullet/V^+)$	$E^\circ(V^-/V^\bullet)$	$E^\circ(Ar/Ar^{+\bullet})$
3a / 4'-OH	+0.59	–1.03(irrev)	+1.8(irrev)
3b / 3'-OH	+0.61	–1.03 (irrev)	+1.8(irrev)
3c / 2'-OH	+0.72	–0.83 (irrev)	+1.87(irrev)
3d / 4'-OCH_3	+0.52	–1.01	+2.0
3e / 3'-OCH_3	+0.56	–1.02	+2.0
3f / 2'-OCH_3	+0.60	–1.04	+2.12(irrev)
3g / 3',4'-$(OH)_2$	+0.58	–1.1 (irrev)	+1.1(irrev)
3h / 3'-(OCH_3)-4'-OH	+0.58	–0.95	+1.1(irrev)
3i / 3',4'-$(OCH_3)_2$	+0.60	–0.95	+1.68
3j / 4'-$N(CH_3)_2$	+0.54	–0.97	+1.1
3j-H^+ / 4'-$NH(CH_3)_2^+$	+0.69		
anisole[a]			+1.75
veratrole[a]			+1.47
dimethylaniline[a]			+0.76
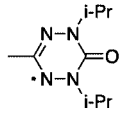	+0.60[c]		
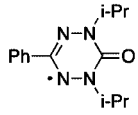	+0.60[d]	–1.08	
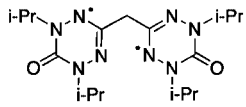	+0.65,+0.75[c]		
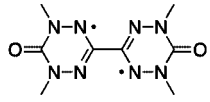	+0.75, +1.01[e]		

[a] From ref 21. [b] From ref 22. [c] From ref 17. [d] From ref 16. [e] From ref 23. [f] Potentials were calibrated with internal ferrocene and reported vs SCE.

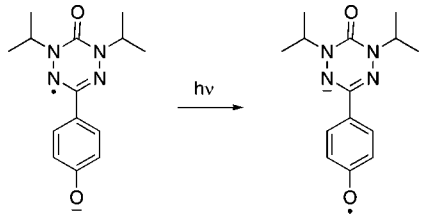

FIGURE 6. Depiction of the charge transfer contribution to the first excited state of the anion of **3a**.

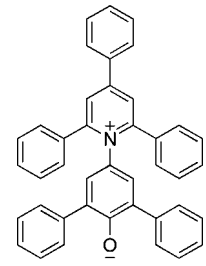

4

increasing contribution from the aryl ring as electron density on the ring is increased.

Several further specific observations are also consistent with this model. For the 2′-hydroxyphenyl verdazyl **3c**, hydrogen bonding between verdazyl and phenol enhances the vibronic structure by increasing the rigidity of the system (Figure 3c solid line). Contrasting this, the 2′-methoxyphenyl-substituted species **3f** absorbs at significantly shorter wavelength and the UV−vis spectrum shows no vibronic structure, consistent with reduced conjugation between phenyl and verdazyl and a larger degree of structural flexibility (Figure 3c, dotted line). Deprotonation of **3c** results in a loss of hydrogen bonding, changing the conformation from a planar to a nonplanar geometry and resulting in a blue shift in the spectrum (Figure 3c, dashed line) rather than the red shift observed upon deprotonation of the 4′-hydroxyphenyl radical **3a** (Figure 3a).

This model of the electronic spectra of oxoverdazyls is also consistent with changes in UV−vis spectra associated with metal

coordination. That the longest wavelength (lowest energy) band is a charge transfer to the verdazyl SOMO fits with the observed ligand dependence in Cu(I) phosphine coordination compounds.[30] The smaller changes in the UV−visible spectrum observed with other reported verdazyl transition metal coordination compounds[11,13,30] point to weaker metal−ligand overlap with these systems.

Conclusion

Because of the node in the SOMO at C3, properties of verdazyls that are dependent largely on the shape and energy of the SOMO (electrochemistry, ESR) are for the most part insensitive to changes in substituents at the 3 position. Nevertheless, properties that also depend upon other orbitals (UV−vis, substituent pK_a) do show some variation. In particular these properties reveal that the verdazyl group is electron withdrawing to an extent comparable with other nitrogen heterocycles and can act as an electron acceptor with sufficiently strong donors.

Experimental Section

General. Tetrazanes and verdazyls were synthesized by using the procedure described by Paré and co-workers.[15] Verdazyls **3a** and **3c** have been reported previously. Other general experimental details are provided in the Supporting Information.

2,4-Diisopropyl-6-(3′-hydroxyphenyl)-1,2,4,5-tetrazane-3-one (2b). 3-Hydroxybenzaldehyde (0.244 g) gave 0.126 g of tetrazane **2a** (23%) with mp 197 °C dec; IR (NaCl) 3244 (N−H), 2967, 2924 (C−H), 1578 (C═O); ^{1}H NMR (300 MHz, DMSO) 1.02 (6H, d, J = 6.6 Hz), 1.05 (6H, d, J = 6.6 Hz). 4.25 (1H, t, J = 11.6 Hz), 4.49 (1H, septet, J = 6.6 Hz), 4.88 (2H, d, J = 11.6 Hz), 6.74 (1H, d, J = 8.1 Hz), 6.98 (2H, m,), 7.18 (1H, t, J = 8.1 Hz), 9.49 (1H, s); ^{13}C NMR (75 MHz, DMSO) 18.3, 19.4, 46.6, 71.4, 113.6, 115.0, 117.0, 129.2, 137.7, 153.4, 157.2; EI-MS *m/z* (rel intensity) 278 (M^+, 55), 163 (100), 120 (95).

1,5-Diisopropyl-3-(3′-hydroxyphenyl)-6-oxoverdazyl (3b). 2,4-Diisopropyl-6-(3′-hydroxyphenyl)-1,2,4,5-tetrazane-3-one (69.5 mg) gave 5.7 mg of verdazyl **2b** (8.3%) with mp 166 °C dec; IR (NaCl) 3291 (O−H), 2978, 2936 (C−H), 1653 (C═O); EI-MS *m/z* (rel intensity) 275 (M^+,63), 191 (100), 120 (37). Anal. Calcd for $C_{14}H_{19}N_4O_2$: C 60.96, H 7.04, N 19.96. Found: C 61.09, H 6.91, N 20.36.

1,5-Diisopropyl-3-(4′-methoxyphenyl)-6-oxoverdazyl (3d). 1,5-Diisopropyl-3-(4′-hydroxyphenyl)-6-oxoverdazyl (41 mg) was dissolved in minimal DMF (ca. 1 mL). Excess (0.2 g) Cs_2CO_3 was added to the solution resulting in a deep purple-blue color. Addition of excess (0.2 mL) CH_3I turned the solution red over a period of ∼5 min. Stirring was continued at room temperature for 30 min after which the solution was diluted with 5 mL of water and extracted with 1 mL of dichloromethane. Evaporation of the dichloromethane gave 39 mg of verdazyl **3d** (90%) as a red crystalline solid with mp 59.6−63.8 °C; IR (NaCl) 2979, 2932, 2875, 2839 (C−H), 1676 (C═O); EI-MS *m/z* (rel intensity) 289 (M^+,40), 205(100), 134(53); EI-MS *m/z* (rel intensity) 289 (M^+,40), 205 (100), 134 (53). Anal. Calcd for $C_{15}H_{21}N_4O_2\cdot 0.3CH_3OH$: C 61.41, H 7.45, N 18.69. Found: C 61.31, H 7.34, N 18.73.

2,4-Diisopropyl-6-(3′-methoxyphenyl)-1,2,4,5-tetrazane-3-one (2e). 3-Methoxybenzaldehyde (68 mg) gave 86.5 mg of tetrazane **5a** (60%) with mp 128.2−128.9 °C; IR (NaCl) 3240 (N−H), 2967, 2932 (C−H), 1602 (C═O); ^{1}H NMR (300 MHz, $CDCl_3$) 1.14 (6H, d, J = 6.6 Hz), 1.16 (6H, d, J = 6.6 Hz), 3.74 (2H, d, J = 12 Hz), 3.84 (3H, s), 4.57 (1H, t, J = 12 Hz), 4.68 (1H, septet, J = 6.6 Hz), 6.90 (1H, dd, J = 8.1, 2.4 Hz), 7.18 (2H, m), 7.33 (1H, t, 7.5); ^{13}C NMR (75 MHz, DMSO) 18.4, 19.5, 47.8, 55.3, 70.9, 112.5, 113.6, 118.2, 129.8, 137.2, 154.3, 159.8; EI-MS *m/z* (rel intensity) 292 (M^+, 74), 177 (84), 134 (100).

1,5-Diisopropyl-3-(3′-methoxyphenyl)-6-oxoverdazyl (3e). 2,4-Diisopropyl-6-(3′-methoxyphenyl)-1,2,4,5-tetrazane-3-one (63.8 mg) gave 46.2 mg of verdazyl **5b** (72%) with mp 87.0−88.2 °C; IR (NaCl) 2980, 2933 (C−H), 1680 (C═O); EI-MS *m/z* (rel intensity) 289 (M^+,66), 205 (100), 134 (32). Anal. Calcd for $C_{15}H_{21}N_4O_2\cdot 0.25CH_3OH$: C 61.62, H 7.41, N 18.86. Found: C 61.69, H 7.78, N 19.02.

2,4-Diisopropyl-6-(2′-methoxy)-1,2,4,5-tetrazane-3-one (2f). 2-Methoxybenzaldehyde (62 mg) gave 120 mg of tetrazane **4a** (82%) with mp 176.4−179.9 °C; IR (NaCl) 3251 (N−H), 2968, 2933 (C−H), 1609 (C═O); ^{1}H NMR (300 MHz, $CDCl_3$) 1.08 (6H, d, J = 6.9 Hz), 1.10 (6H, d, J = 6.9 Hz), 3.89 (3H, s), 4.38 (1H, t, J = 12.0 Hz), 4.67 (2H, d, J = 12.0 Hz), 4.69 (1H, septet, J = 6.9 Hz), 6.96(1H, dd, J = 1, 8.3 Hz), 7.01 (1H, td, J = 1, 7.5 Hz), 7.25 (1H, dd, J = 1.8, 7.5 Hz), 7.35 (1H, ddd, J = 1.8, 7.5, 8.3 Hz); ^{13}C NMR (75 MHz, $CDCl_3$) 18.3, 19.4, 47.7, 55.5, 74.0, 111.4, 121.6, 123.4, 130.2, 130.3, 153.9, 157.0; EI-MS *m/z* (rel intensity) 292 (M^+, 53), 177 (74), 134 (100).

1,5-Diisopropyl-3-(2′-methoxy)-6-oxoverdazyl (3f). 2,4-Diisopropyl-6-(2′-methoxyphenyl)-1,2,4,5-tetrazane-3-one (99 mg) gave 68.9 mg of verdazyl **4b** (70%) with mp 100.3−102.4 °C; IR (NaCl) 2994, 2974 (C−H), 1676 (C═O); EI-MS *m/z* (rel intensity) 289 (M^+, 100), 205 (89). Anal. Calcd for $C_{15}H_{21}N_4O_2$: C 62.28, H 7.27, N 19.38. Found: C 62.03, H 7.32, N 19.05.

2,4-Diisopropyl-6-(3′,4′-dihydroxyphenyl)-1,2,4,5-tetrazane-3-one (2g). 3,4-Dihydroxybenzaldehyde (138 mg) gave 195 mg of tetrazane **7a** (66%) with mp 218.2−226.9 °C; IR (NaCl) 3237 (N−H), 2968, 2932 (C−H), 1584 (C═O); ^{1}H NMR (300 MHz, dmso-d_6) 0.97 (6H, d, J = 6.7 Hz), 1.01 (6H, d, J = 6.7 Hz), 4.11 (1H, t, J = 12.1 Hz), 4.43 (2H, septet, J = 6.0 Hz), 4.76 (2H, d, J = 11.7 Hz), 6.69 (1H, d, J = 8.1 Hz), 6.76 (1H, dd, J = 8.4, 1.8 Hz), 6.90 (1H, ds, J = 1.8 Hz); ^{13}C NMR (75 MHz, dmso-d_6) 18.8, 19.9, 47.2, 71.8, 114.7, 115.7, 117.8, 127.8, 145.4, 145.8, 154.0; EI-MS *m/z* (rel intensity) 294 (M^+, 50), 179 (40), 136 (100).

1,5-Diisopropyl-3-(3′,4′-dihydroxyphenyl)-6-oxoverdazyl (3g). 2,4-Diisopropyl-6-(3′,4′-dihydroxyphenyl)-1,2,4,5-tetrazane-3-one (170 mg) gave 85 g of verdazyl **7b** (50%) recrystallized from methanol/water to give a red solid with mp 190 °C dec; IR (NaCl) 3330 (O−H), 2979, 2932 (C−H), 1648 (C═O); EI-MS *m/z* (rel intensity) 291 (M^+, 65), 207 (100), 136 (67), 135 (64). Anal. Calcd. for $C_{14}H_{19}N_4O_3\cdot 0.3CH_3OH$: C 57.02, H 6.74, N 18.57. Found: C 57.18, H 6.59, N 18.26.

2,4-Diisopropyl-6-(3′-methoxy-4′-hydroxyphenyl)-1,2,4,5-tetrazane-3-one (2h). 3-Methoxy-4-hydroxybenzaldehyde (77 mg) gave 100.2 mg of tetrazane **8a** (65%) with mp 173.6−175.7 °C; IR (NaCl) 3247 (N−H), 2970, 2935 (C−H), 1607 (C═O); ^{1}H NMR (300 MHz, $CDCl_3$) 1.15 (6H, d, J = 6.5 Hz), 1.16 (6H, d, J = 6.5 Hz), 3.70 (2H, d, J = 12.1 Hz), 3.93 (3H, s), 4.54 (1H, t, J = 12.1 Hz), 4.69 (2H, septet, J = 6.5 Hz), 5.85 (1H, ds, J = 9.1 Hz), 6.93 (1H, d, J = 9.0 Hz), 7.07 (2H, m); ^{13}C NMR (75 MHz, $CDCl_3$) 18.4, 19.6, 47.7, 56.0, 70.9, 109.0, 114.4, 118.8, 127.6, 146.1, 146.6, 154.4; EI-MS *m/z* (rel intensity) 308 (M^+, 32), 193 (37), 150 (100).

1,5-Diisopropyl-3-(3′-methoxy-4′-hydroxyphenyl)-6-oxoverdazyl (3h). 2,4-Diisopropyl-6-(3′-methoxy-4′-hydroxyoxyphenyl)-1,2,4,5-tetrazane-3-one (77.8 mg) gave 57.4 mg of verdazyl **8b** (73%) with mp 129.5−131.4 °C; IR (NaCl) 2282 (O−H), 2976, 2937 (C−H), 1769 3(C═O); EI-MS *m/z* (rel intensity) 305 (M^+, 58), 221 (100), 150 (47). Anal. Calcd for $C_{15}H_{21}N_4O_3$: C 59.02, H 6.89, N 18.36. Found: C 58.75, H 7.00, N 18.12.

2,4-Diisopropyl-6-(3′,4′-dimethoxyphenyl)-1,2,4,5-tetrazane-3-one (2i). 3,4-Dimethoxybenzaldehyde (83 mg) gave 91.6 mg of tetrazane **9a** (57%) with mp 117.3−119.8 °C; IR (NaCl) 3244 (N−H), 2963, 2917, 2848 (C−H), 1609 (C═O); ^{1}H NMR (300 MHz, DMSO) 1.15 (6H, d, J = 6.3 Hz), 1.16 (6H, d, J = 6.3 Hz), 3.70 (2H, d, J = 12.0 Hz), 3.891 (3H, s), 3.913 (3H, s), 4.56 (1H, t, J = 12.0 Hz), 4.69 (2H, septet, J = 6.3 Hz), 6.88 (1H, d, J = 8.4

(30) Brook, D. J. R.; Abeyta, V. *J. Chem. Soc., Dalton Trans.* **2002**, 4219–4223.

Hz), 7.13 (2H, m); ^{13}C NMR (75 MHz, $CDCl_3$) 154.4, 149.4, 149.0, 128.2, 118.1, 111.0, 109.6, 70.8, 55.9, 47.7, 19.5, 18.4. Note that the two methoxy carbons have fortuitously identical chemical shifts. This was demonstrated by using HETCOR (see the Supporting Information); EI-MS *m*/*z* (rel intensity) 322 (M^+, 42), 207 (39), 164 (100).

1,5-Diisopropyl-3-(3′,4′-dimethoxyphenyl)-6-oxoverdazyl (3i). 2,4-Diisopropyl-6-(3′,4′-dimethoxyphenyl)-1,2,4,5-tetrazane-3-one (80 mg) gave 68.9 mg of verdazyl **9b** (70%) with mp 119 °C; IR (NaCl) 2963, 2917 (C−H), 1668 (C═O); EI-MS *m*/*z* (rel intensity) 319 (M^+, 68), 235 (100), 164 (47). Anal. Calcd for $C_{16}H_{23}N_4O_3$: C 60.19, H 7.21, N 17.55. Found: C 59.99, H 7.37, N 17.40.

2,4-Diisopropyl-6-(4′-dimethylaminophenyl)-1,2,4,5-tetrazane-3-one (2j). 4-Dimethylaminobenzaldehyde (175 mg) gave the corresponding tetrazane recrystallized from heptane (161 mg, 45%): mp 207−208 °C; ^{1}H NMR (300 MHz $CDCl_3$) 7.41 (d, 2H, J = 8.1 Hz), 6.73 (d, 2H, J = 8.1 Hz), 4.70 (septet, 7H, J = 6.6 Hz), 4.511 (t, 1H, J = 12 Hz), 3.65 (d, 2H, J = 12 Hz), 2.97 (s, 6H), 1.16 (d, 6H, J = 6.6 Hz), 1.14 (d, 6H, J = 6.6 Hz); ^{13}C NMR (75 MHz $CDCl_3$) 154.3, 150.7, 126.8, 123.1, 112.2, 70.8, 47.7, 40.4, 19.5, 18.4; IR (NaCl plate) 3239 (NH), 2967, 2928, 1613 (C═O); EI-MS *m*/*z* (rel intensity) 305 (M^+, 20), 190 (19), 148 (50), 147 (100).

1,5-Diisopropyl-3-(4′-dimethylaminophenyl)-6-oxoverdazyl (3j). Oxidation of tetrazane **10** (161 mg) with benzoquinone (85 mg, 1.5 equiv) in hot toluene for 15 min gave 97 mg (61%) of the verdazyl as a greenish-black solid after recrystallization from methanol−water: mp 123−124 °C; IR (NaCl plate) 2975, 2931, 2873, 1677 (C═O); EI-MS *m*/*z* (rel intensity) 302 (M^+, 50), 246 (30), 218 (80), 147 (90), 146(100), 145 (95). Anal. Calcd for $C_{15}H_{24}N_5O$: C 63.58, H 7.95, N 23.18. Found: C 63.25, H 8.02, N 22.84.

Acknowledgment. This research was supported in part by San Jose State University. We also thank the Santa Clara University Chemistry Department for access to their X-ray diffractometer and Dr. Michael Ruf for additional help with collection of single-crystal X-ray data.

Supporting Information Available: Thermal ellipsoid plots and full details of crystallographic data collection for verdazyls **3a**,**f** in cif format, UV−visible spectra for radicals **3d**,**e**,**g**−**i**, tables of ESR data for **3b**,**d**−**j**, ^{1}H NMR and ^{13}C NMR spectra for all new tetrazanes (**2b**,**d**−**j**), GCMS traces for verdazyls **3b**,**d**−**f**,**h**−**j**, HPLC traces for verdazyl **3b**,**d**−**j**, and plot of phenol pK_a in 80% methanol vs Hammett σ constant used to determine Hammett constants for the verdazyl substituent. This material is available free of charge via the Internet at http://pubs.acs.org.

JO8019829